Covalently Bound Humin-Lignin Hybrids as Important Novel Substructures in Organosolv Spruce Lignins

Petter Paulsen Thoresen[†], Heiko Lange[†,‡,*], Ulrika Rova[†], Paul Christakopoulos[†], Leonidas Matsakas[†,*]

[†] *Biochemical Process Engineering; Division of Chemical Engineering; Department of Civil, Environmental and Natural Resources Engineering; Luleå University of Technology, 971-87, Sweden*

[‡] *Department of Earth and Environmental Sciences, University of Milano-Bicocca, Piazza della Scienza 1, 20126 Milan, Italy*

***Author for correspondence:**

Associate Prof. Heiko Lange, Department of Earth and Environmental Sciences, University of Milano-Bicocca, Piazza della Scienza 1, 20126 Milan, Italy, heiko.lange@unimib.it, +39 02 6448 2824

Associate Prof. Leonidas Matsakas, Department of Civil, Environmental and Natural Resources Engineering, Luleå University of Technology, 971 87 Luleå, Sweden, leonidas.matsakas@ltu.se, +46 (0) 920 493043.

Highlights

- Spruce lignins were isolated via a steam-explosion organosolv process.
- Isolated lignins were analysed for structural features and thermal stabilities.
- Data suggest that covalently linked lignin-humin hybrids are eventually formed.
- Thermal stability profiles sustain the presence of such hybrid structures.

Abstract

Organosolv lignins (**OSLs**) are important byproducts of the cellulose-centred biorefinery that need to be converted in high value-added products for economic viability. Yet, **OSLs** underperform. Applying advanced NMR, GPC, and thermal analyses, isolated spruce lignins were analysed to correlate organosolv process severity to the structural details for delineating potential valorisations. Very mild conditions were found to not fractionate the biomass, causing a mix of sugars, lignin-carbohydrate complexes (**LCCs**), and corresponding dehydration/degradation products and including pseudo-lignins. Employing only slightly harsher conditions promote fractionation, but also formation of sugar degradation structures that covalently incorporate into the oligomeric and polymeric lignin structures, causing the as organosolv lignin isolated materials to represent de facto lignin-humin hybrid (**HLH**) structures not yet evidenced as such in organosolv lignins. These structures effortlessly explain observed unexpected solubility issues and unusual thermal responses, and their presence might have to be acknowledged in downstream lignin valorisation.

Keywords

humins, organosolv lignin, structure elucidation

1 Introduction

A multitude of industrial chemicals and materials are generated from petroleum-based platform chemicals as they serve as starting points for commercially important polymers, construction material, composites, fibres, etc.[1,2] In light of the urgency of finding a replacement for the petroleum-based platform chemicals, lignocellulosic material is considered a promising source, while also holding the potential of net zero carbon profiles.[1] As recently reviewed, both the C5 and C6 sugars from hemicellulose and cellulose, as well as their derivatives have potential as building block chemicals with industrial applications.[1] Lignin, representing a significant portion of lignocellulosic biomass, holds a high, but yet rather unutilized potential, being the largest renewable resource of aromatics, and being produced at a quantity of 50 million tons per year at the moment, with only 2% of this amount being commercially exploited. Suitable downstream applications of isolated lignins depend on structural features of the lignin of choice, and thus both on the source of the lignocellulosic raw material and on the mode of extraction, since both factors are determining for the structural features of the eventually isolated lignins. For softwoods, guaiacyl units dominate over traces of syringyl and p-hydroxylcinnamyl units in terms of abundance within the lignin, being engaged mainly in the four most frequently occurring motifs, *i.e.*, β-ethers (60%), dibenzodioxocin (9-12%), phenylcoumaran (10%) and resinol (5%) motifs; these are accompanied by traces of biphenyl ethers (1%) and spirodienones (1-2%).[3] Due to the radical-driven biosynthesis of lignin presumably lacking stringent control mechanisms, the distribution of these motifs is random in terms of combinations of the different motifs alongside branched and/or linear chains of varying molecular weights. Both alkaline and acidic systems can be principally applied to fractionate lignocellulosic biomass into the three main polymer streams, *i.e.*, cellulose, hemicelluloses and lignin,[4] to furnish starting points for downstream valorisations that target aspects that are not available by valorisation strategies like pyrolysis that use unfractionated biomass. Naturally, the different inter-unit linkages in lignin will display different susceptibilities towards different chemical treatments[5] and thus affect the structural and hence chemical and physical properties of the polyphenolic end-isolate, including solubility, thermal stability, reactivity profile, etc.[6]

Mechanical pretreatments are often applied alongside suitable chemical systems with or without addition of catalysts to increase overall fractionation efficiency. A physical mode often applied to the fractionation of lignocellulosic material is steam explosion (**SE**), with this method primarily applied for the depolymerisation of hemicellulose and the extraction of sugar species.[7] This means of pretreatment benefits from mechanical and thermal conditions, and the entire structure is softened and easier distorted.[8]Among the most promising chemical methods for fractionation of lignocellulosic biomass are the organosolv (**OS**) processes. Their application in form of EtOH in an

aqueous system with or without mineral acid catalyst has previously been applied for fractionation of the highly recalcitrance softwoods such as spruce.[9–12]

As of now only few works investigated combinations of two promising modes of pretreatment, *i.e.*, **SE-OS** processes, with respect to potential synergies and the impact of variations in process parameters such as time and acidity on the characteristics of the resulting lignin isolates, and thus the suitability for potential downstream valorisations.[13] The present work set out to investigate the fractionation of spruce through a combined **SE-OS**, looking at the most important process parameters time and intrinsic acidity, as well as their reflection in the structural features of the isolated polyphenols and observed fundamental macroscopic properties.[14]

3 Results and discussion

3.1 Lignin isolation and structural aspects

The **SE-OS** treatment conditions applied for isolating six spruce organosolv lignins are listed in Table 1, together with obtained solubilisations of lignins. Quantitative ^{31}P NMR, quantitative ^{13}C NMR and semiquantitative HSQC analyses as well as gel permeation chromatography results were employed in order to elucidate the structural characteristics for the various isolated lignins (Table 1). Listed motifs, structurally depicted in case of lignin structural features in Figure 1, and in case of humin-type structures in Figure 3, were identified on the basis of literature reports. [15–23]
It is important to note that the HSQC-derived data shown in the table, albeit being semiquantitative, allow for the delineation of the discussed relative trends on the basis of a comparable amount of lignin analysed for each sample and the standardised sample preparations.

Table 1: Extraction conditions, yields, abundances of key structural motifs, molecular weights, and monomer compositions for the lignins isolated under the various **SE-OS** process conditions. Data derived from non-quantitative HSQC measurements were normalised in semiquantitative fashion on the basis of the G-2H-signal. Quantitative ^{13}C NMR was analysed on the basis of the internal standard trioxane. Error for ^{13}C NMR quantification data was estimated to be ±0.2 mmol/g.

Lignin sample	**S1**	**S2**	**S3**	**S4**	**S5**	**S6**	**NMR shifts[a]**	**ref [b]**
Process conditions								
T [°C]	200	200	200	200	200	200		
duration [min]	15	30	60	30	30	30		
ethanol content [%v/v]	65	65	65	52	52	52		
sulfuric acid content [%w/w]	0	0	0	0	0.2	1.0		
Solubilised lignin (Klason) [% w/w][c]	50.8	71.7	61.9	76.2	71.8	79.4		
Lignin - interunit binding motif (HSQC)	**Abundance [%C9 (semiquantitative)]**							
β-*O*-4' (average $C^{\alpha\beta}$-H) (**A**)	8.21	3.20	3.42	3.94	3.62	2.78	4.78|71.1 4.31|83.3	[24,25]
α-ethoxylated β-*O*-4' linkage (C^{α}-H) (**B**)	3.64	4.25	7.25	6.28	4.69	0.00	4.50|79.7	[26]
α-oxidised β-*O*-4' linkage (C^{α}-H) (**C**)	0.46	0.87	0.53	0.97	0.99	0.85	5.63|88.0	[26]
β-β' (average $C^{\alpha\beta}$-H) (**D**)	2.39	1.73	1.26	2.67	2.43	1.95	4.62|84.9 3.06|53.5	[24]
β-5' (average $C^{\alpha\beta\gamma}$-H) (**E**)	4.99	6.31	6.43	6.95	6.82	5.91	5.45|86.9	[24,27]
β-1' (**F**)	5.69	0.98	0.05	2.01	2.09	2.06	3.60|51.9	[25]
secoisolariciresinol (**G**)	1.10	1.27	1.42	0.00	1.33	0.89	2.52|33.7 1.87|42.3	[28]
total interunit motifs	*26.5*	*14.4*	*17.5*	*22.8*	*22.0*	*14.4*		
G units (average of $C^{2.5}$-H)	99.4	99.2	97.6	99.0	96.2	98.1	6.93/|10.2 6.77/|15.2	[24,29]
Lignin - end groups (HSQC)	**Abundance [%C9 (semiquantitative)]**							
Hibbert ketone, C^{γ}-H (**H**)	0.32	0.85	0.28	0.32	0.52	0.56	3.64|44.1	[30]
coniferyl aldehyde (aver. of $C^{\alpha\beta}$-H) (**J**)	0.66	0.65	0.73	0.91	1.02	0.66	7.42|125.8	[29]
coniferyl alcohol ($C^{\alpha\beta\gamma}$-$H^{\alpha\beta\gamma}$) (**K**)	1.50	0.66	1.08	1.15	1.24	0.25	6.43|131.4 6.14|130.6	[24]
guaiacyl propanol (**L**)	2.10	2.19	2.07	2.15	2.47	1.76	2.53|31.2 1.69|34.4	[28]
guaiacyl acetic acid (**M**)	0.06	0.32	0.09	0.07	0.19	0.08	3.63|38.1	[30]
guaiacyl hydroxy-acetic acid (C^{α}-H) (**N**)	0.32	0.44	0.25	0.28	0.32	0.29	4.90|75.6	[31]
guaiacyl aldehyde (CHO) (**O**)	0.43	0.55	0.51	0.79	1.07	0.45	9.58|28.9	[32]
….total end groups	*5.39*	*5.66*	*5.01*	*5.67*	*6.83*	*4.05*		
Lignin - OH-groups (^{31}P NMR)	**Abundance [mmol/g]**							
aliphatic OH	3.04	3.17	2.55[d]	2.97[e]	2.47	2.42	145.5-150.0	[33]
C_5-subst./condensed guaiacylic OH	0.34	0.25	0.69[d]	0.85[e]	0.42	0.36	144.7-140.0	[34]
guaiacyl OH	0.87	1.16	1.29[d]	1.47[e]	1.56	1.42	139.0-140.0	[34]
p-hydroxyphenol OH	0.09	0.03	0.09[d]	0.13[e]	0.06	0.05	137.3-138.2	[34]
carboxylic acid OH	0.21	0.16	0.12	0.18	0.12	0.12	133.6-136.6	[34]
total phenolic OH	*1.30*	*1.44*	*2.07[d]*	*2.45[e]*	*2.04*	*1.83*		
G-OH/condensed OH	*2.56*	*4.64*	*1.87*	*1.73*	*3.71*	*3.94*		
arom-OH/ali-OH	*0.43*	*0.45*	*0.81*	*0.83[b]*	*0.83*	*0.76*		

Lignin – add. funct. motifs (^{13}C NMR)	**Abundance [mmol/g]**							
Ar-CHO	0.26	0.55	0.93	0.99	0.33	0.00	191.0	[35]
quaternary C ('C^{q}')	67.2	64.8	101	80.0	151	38.2	132.0-160.0	[36]
tertiary C ('C^{t}')	106	226	142	121	63.2	53.2	132.0-100.0	[36]
C_t/C_q	*0.63*	*0.29*	*0.72*	*0.66*	*2.39*	*0.72*		
aromatic C-H	89.0	80.5	81.4	73.9	101	34.4	125.0-96.0	[15]
LCCs (HSQC)	**Abundance [%C9 (semiquantitative)]**							
benzyl ether ($C^{\alpha,\beta}$-H in β-*O*-4') (**P**)	1.19	1.40	0.85	0.00	0.00	0.00	4.55|80.2	[37]
phenyl glycoside ($C^{1,2}$-H) (**Q**)	0.90	0.03	0.00	0.04	0.02	0.00	4.72|100.7 3.12|77.2	[38]
alkyl glycoside (C^{γ}-H) (**R**)	6.81	0.10	0.22	0.41	0.15	0.09	3.06|69.9	[38]
Furfural and humins – functional groups (HSQC)	**Abundance [%C9 (semiquantitative)]**							
furan-*CH*$^{\beta}$ (**I**)	2.93	1.29	1.18	0.81	0.79	0.79	7.48|124.3	[16]
furfural *CH*O (**I**)	1.34	0.39	0.13	0.03	0.17	0.08	9.57|12.7	[17]
5-HMF-CH_2R (**I**)	1.48	0.63	0.45	0.37	0.40	2.19	4.52|55.7	[16]
R-CH_2C(O)C$H_2CH_2CO_2$H (**IX**)	1.36	1.21	1.47	1.37	1.39	1.27	2.00|26.4 2.19|33.4	[16]
furan-benzyl ether (C^{α}-H) (**X**)	0.22	0.55	0.39	0.44	1.04	0.39	4.56|68.0	
oxiran-C^4H (**XI**)	5.40	1.10	1.60	1.56	1.40	0.99	5.24|71.4	[16]
oxiran-C^6H (**XI**)	4.91	1.48	1.65	2.60	2.46	2.45	4.18|66.9	[16]
furan – phenol methylene bridge (**XIII**)	6.68	1.70	2.14	0.83	1.00	0.43	3.45|56.0	[18]
Furfural and humins – functional groups (^{13}C NMR)	**Abundance [mmol/g]**							
furfural C^5 (**I**)	0.01	0.01	0.01	0.01	0.00	0.00	152.0	[18]
furfural *C*HO (**I**)	3.58	21.4	0.00	9.00	0.36	0.00	178.0	[17]
furan biaryl *via* C^{β}- C^{β} (**III**)	0.00	0.00	0.66	0.00	0.00	0.00	127.0	[19]
*C*3 in polyfuran motif (**VII**)	11.1	10.3	8.36	8.90	4.47	3.33	110.0	[19]
'opened' furan *C*=O (**VIII**)	1.99	7.66	0.00	3.28	0.00	0.00	208.0-205.0	[15]
furan-phenol biaryl *via* C^{α}- C^5 (**XII**)	11.2	11.7	11.9	12.6	4.47	2.22	105.9	[20]
Pseudo-lignin – functional groups (^{13}C NMR)	**Abundance [mmol/g]**							
R-CH_2-CHO	2.15	15.6	0.00	7.00	0.25	0.00	43.0	[21]
Ar-*C*H_2-Ar	2.15	3.30	4.15	3.04	2.06	1.80	29.0-42.0	[22]
Ar-*C*-O-R	1.33	0.00	0.44	0.00	0.00	1.33	167.0	[39]
Molecular weight (GPC)								
Mn [kDa]	1.0	1.2	1.5[d]	1.0[e]	1.2	1.4		
Mw [kDa])	9.0	7.5	6.3[d]	2.8[e]	3.7	6.1		
polydispersity index (Mw/Mn)	8.90	6.28	4.29[d]	2.79[e]	2.96	4.36		
Lignin aromatic units (py-GC)	**Abundance (%)**							
S	1	1	1	1[e]	1	2		
G	94	93	93	91[e]	93	91		
H	5	6	6	7[e]	6	8		

[a] Shifts actually used for analysis in δ(^{1}H)/[ppm] | δ(^{13}C)/[ppm] for HSQC data, and in δ(^{13}C)/[ppm] for ^{13}C NMR data.

[b] References used as guide/comparison for shifts.

[c] Data previously published.[40]

[d] Data previously published.[41]

[e] Data previously published.[42]

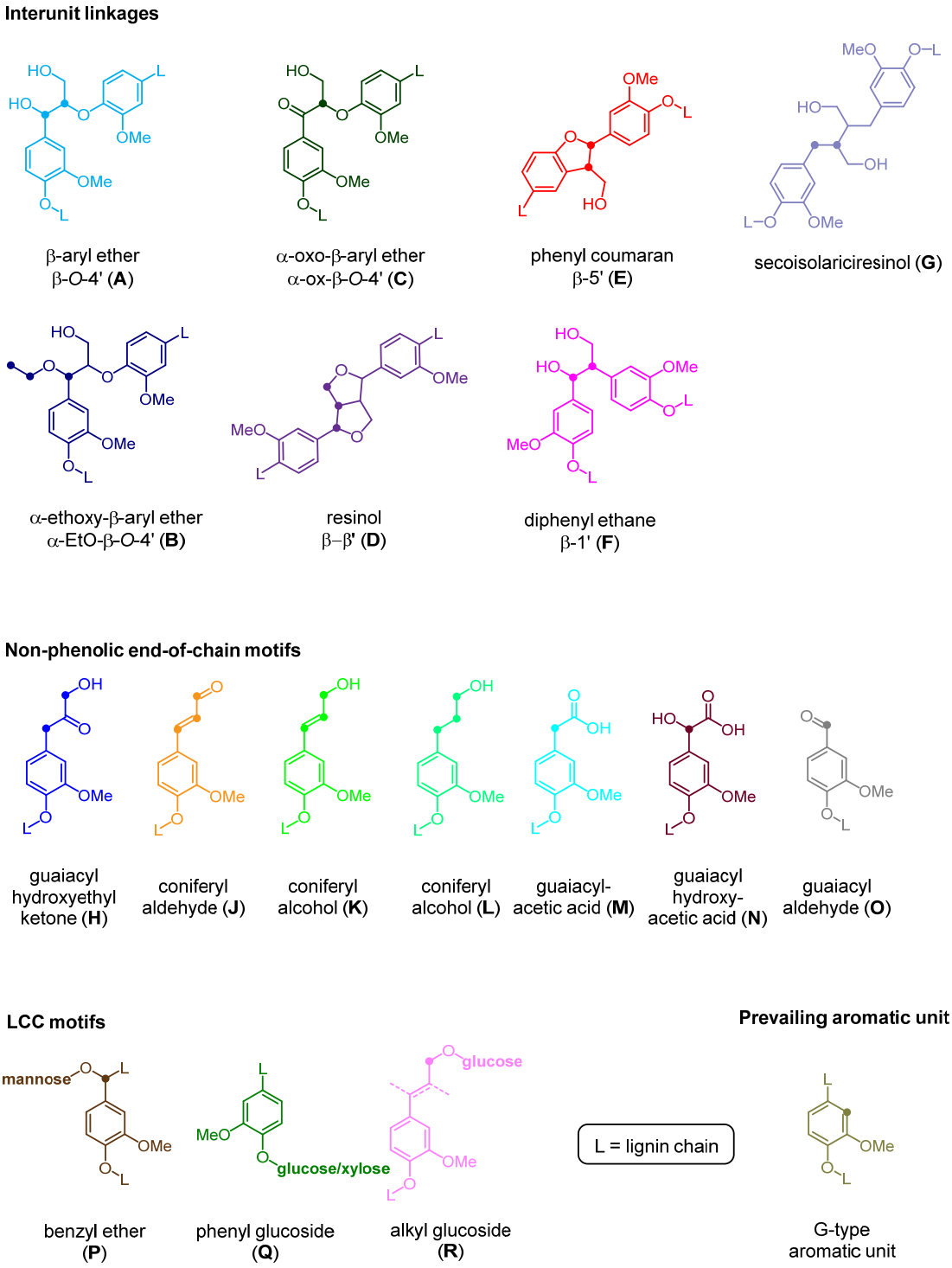

Figure 1. Important structural motifs of lignins unambiguously identified in the analyses of the HSQC and ^{13}C NMR spectra of lignins **S1** – **S6**. Colour coding matches that used in Figure 2.

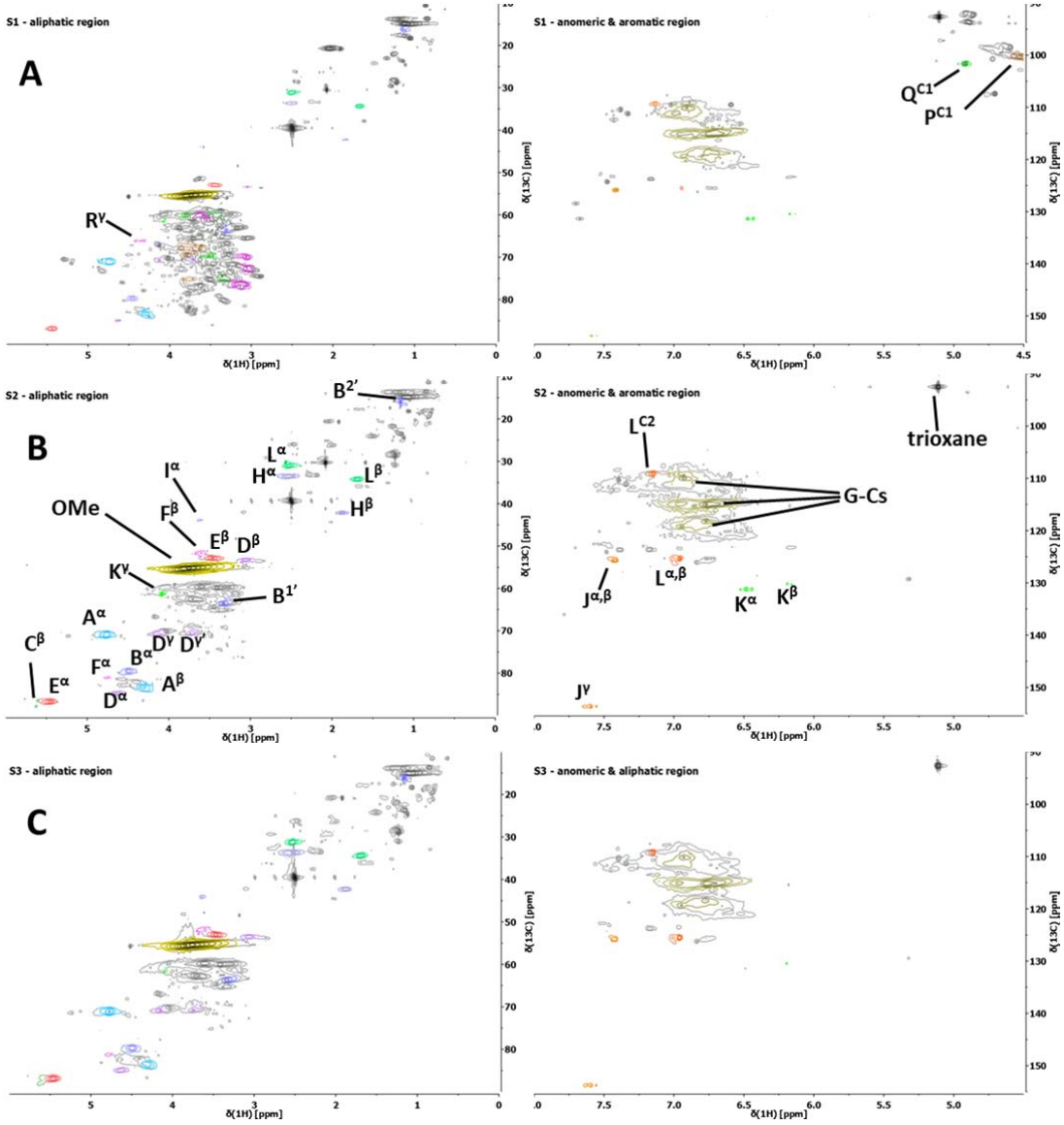

Figure 2. HSQC spectra of the isolated lignins, split in aliphatic and anomeric/aromatic regions. Key structural motifs were colour-coded following colours used in Figure 1: (A) **S1**; (B) **S2**; (C) **S3**.

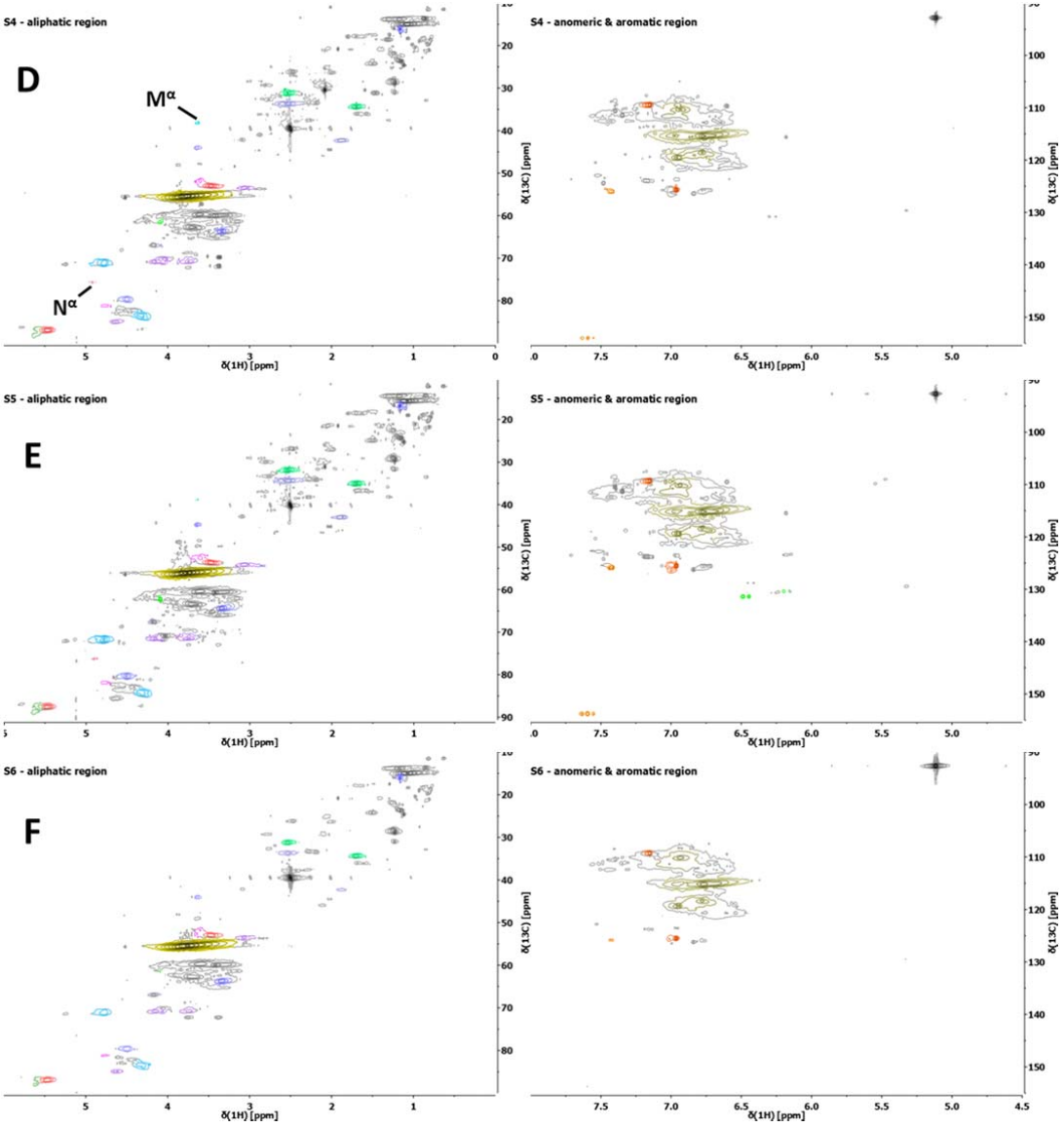

131

132 ***Figure 2 continued.*** HSQC spectra of the isolated lignins, split in aliphatic and anomeric/aromatic regions. Key
133 structural motifs were colour-coded following colours used in Figure 1: (D) **S4**; (E) **S5**; (F) **S6**.

134

135

136

3.2 Effect of treatment time (samples S1, S2, and S3)

Differences in treatment conditions strongly affect the amount of the as lignin isolated material (Table 2), indicating essentially changes in fractionation efficacy, introduced changes in physico-chemical behaviours, and thus eventually also in the structure of the isolated material.

Detailed structural analysis of **S1** by HSQC, including an semiquantitative analyses of the signals confirms an insufficient fractionation, leaving significant amounts of carbohydrates in the isolated lignin fraction (Figure 2A). Studies suggest that in coniferous species the lignin is significantly bound to the hemicellulose through lignin carbohydrate complexes (**LCCs**);[43] yet, as recently reviewed,[5] the exact nature and extent of these LCCs is still pending. Postulated binding motifs include benzyl ether (BE), phenyl glycosidic (PG), and γ-ester (GE) linkages involving galactoglucomannan and arabinoglucuronoxylan;[37] alkyl glucosides have also been claimed.[38] In lignin **S1**. α-benzyl ethers (**P**, Figure 1) are present at a content of 1.19 mmol/g (average over C^{α} and C^{β} in β-*O*-4'); phenylglucosides (**Q**) were identified and quantified to 0.90 mmol/g (average over C^{1}, C^{2}), and alkylglucosides (**R**) were identified in significant amounts (average over C^{γ}, C^{4}). The signals of the expectable carbohydrates commonly linked to these motifs are accompanying the cross-peaks seen as indicative of **LCCs** (Figure 2A), forming together hence a hallmark of insufficient process severity. Correspondingly, anotable reduction of these groups is seen in **S2** upon extended reaction times. Coniferyl alcohol (**K**, Figure 1) interestingly drops with slightly higher process intensity as well in **S2**; its appearance can be interpreted as indicative of an onset of cleavage of eventually present alkyl glucuronic acid ester linkages. The fact that the abundance of this motifs is present in all samples, in combination with the fact that alkyl glucuronic acid ester linkages could not reliably be detected in **S1** as a fourth **LCC** motif, suggest that **S1**-conditions were strong enough to cleave at least parts of presumable **LCCs**. The constant presence of the group renders it less probable that the motif emerges as an onset of dehydrating decomposition of corresponding hydroxylated endgroups.

The amount of aromatic C-H augments with increasing treatment time. While increase from **S1** to **S2** is explained at least in part by removal of dilution effects caused by the carbohydrate impurities, the increase also reflects a more efficient biomass fractionation, liberating more and larger lignin molecules/fragments from the various cell walls going from **S2** to **S3**. ^{31}P NMR data (Table 1) reveal a concomitant slight increase in aliphatic OH-groups, despite the *de facto* elimination of sugar-based aliphatic OH-groups. Considering that the increase in G-type phenolic OH-groups (Table 2) is more pronounced, depolymerisation under cleavage of internal lignin ether linkages seems likely as commencing depolymerisation process. [34,44] This interpretation is supported by the gradual increase in lignin end-groups (Table 1). At the same time, intensities of signals C^{α}-H and C^{β}-H in

ethoxylated β-*O*-4' motifs augment from **S1** to **S2** (Table 1). This known [26] benzylic alkoxylation shows in the context of the ethanosolv conditions an S_N-type cleavage of benzyl ether **LCC**-motifs that displays a preserving effect on β-*O*-4' structures, leading to the extraction of by tendency larger lignin molecules under **S2** conditions.[45] This interpretation is sustained by the decrease in the polydispersity index (PDI) when doubling extraction time in combination with a small net increase in the number average molecular weight (Mn) (Table 1).

Reaction times of 60 min for production of **S3** lead to a decline of both the extractable amount of lignin and its structural integrity. The formation condensed structures is also indicated by the ^{31}P NMR data, with the content of condensed aromatic OH-groups doubling alongside a decrease in aliphatic OH-groups. The decrease in total abundance of endgroups for **S3**, irrespective of relative changes among them, indicates together with GPC data also an onset of repolymerisation of initially smaller fragments stemming from a successful decomposition as potentially indicated by the decreased M_w of **S3**. The latter might also be interpreted, however, as a more effective re-deposition of eventually structurally changed lignin molecules on fibrous surfaces, causing consequently the observed reduced extraction yield.[13]

3.3 Effect of ethanol content (samples S2 and S4)

Adjusting solvent composition is a common lever for tuning system reactivity in OS processes.[13] Based on interesting recent works that allow for a discussion of organosolv pretreatments as a function of solvent composition, [46,47] it was speculated that especially the degree of a disturbance of the intrinsic water structure would increase system activity, generating an environment where certain reactions occur to a greater extent through enhanced stabilization of transition states and more active catalytic components: improved aqueous hydration of rather hydrophobic ethanol clusters in the media[48] might generate a more reactive system through elevated proton activity due to the role of the hydroxyl to hydrate in said hydrophobic clusters.[49] EtOH-concentration was lowered from 65% v/v to 52% v/v for the production of lignin **S4**, using otherwise **S2** conditions.

The lower EtOH content for **S4** leads to a higher content of solubilized lignin, eventually due to a very efficient biopolymer fractionation and a reduction of re-polymerisation and re-deposition, which is turn is likely the result of the decreased hydrophobic aggregation and which has been found dependent on the available surface area of non-polar structures, [46] eventually inform of ethoylated β-aryl ethers. The β-*O*-4' content in **S4** is only slightly higher when compared to **S2**, with 3.94 *vs*. 3.20 mmol/g, respectively. As mentioned previously, these relatively stable contents under eventually intrinsically more acidic conditions can originate from protective C^{α}-ethoxylation, which is

abundantly present in **S4** (Table 1). Ethoxylation explains also that the overall increase in aliphatic interunit linkages is represented in the ^{31}P NMR data for **S4** in form of a marginal reduction instead of a slight increase. Interestingly, however, ^{31}P NMR data reveal also an increased content of *ortho*-disubstituted phenols when transiting from higher to lower EtOH concentration, indicative of commencing condensation reactions. This is seen, however, along an invariant total abundance of end-groups in **S4** with respect to **S2**. Since both the number and weight average molecular weight significantly decrease for **S4** (Table 1), a more complex reactive situation in which depolymerisation events and repolymerisations exist in advantageous equilibrium is most likely encountered. Overall, **S4** conditions appear as milder, but well working context for efficient biomass fragmentation.

3.4 Effect of acidic catalyst (samples S4, S5, and S6)

While having an effect on the hydrophilicity/lipophilicity of the system, varying ethanol contents causes changes in system acidity. A blunter, widely applied way of acidity adjustment in (**SE-**)**OS** systems is, however, the addition of catalytic amounts of a mineral acid, a series of biomass fractionations was run in which different loadings of sulfuric acid were applied while keeping otherwise the 30 minutes reaction time and 52% ethanol concentration, with the aim to elucidate more explicitly the role of the acidic environment often applied.[50]

Spectroscopic analysis suggests a significant effect of the acid presence on both amount and structure of isolated lignins **S5** and **S6** compared to **S4**, as discussed in detail in the Supporting Information (Table 1). Holistically, structural data obtained for the acid series suggest a degradation and eventual repolymerisation of the natural lignin as function of system acidity. In front of this rather clear picture, interestingly, lignin solubility sees an initial drop from **S4** to **S5**, before peaking in absolute terms under **S6** conditions. Degradation and re-polymerisation under maximum acidic conditions does thus not seem to lead to re-deposition on fibrous surfaces or insoluble structures.

3.5 Furfural-lignin-hybrid and humin-lignin-hybrid structures

SE-OS related decomposition of hemicelluloses inevitably leads to the presence of carbohydrates and derivatives thereof in the reaction mixture. Further decomposition of the sugar units has been reported, to form furfural and its derivatives in the reaction mixtures. [51,52] Formation of so-called pseudo-lignins has been discussed as larger molecular structures stemming from the re-polymerisation of these reactive sugar degradation products; these larger molecules behave during lignin isolation like lignin, *i.e.*, present a certain acid insolubility, and cause thus as byproducts of

pretreatments issues, both in the quantitative discussion of the isolated lignin quantity with respect to the Klason lignin content of the starting biomass, and thus importantly with respect to a downstream biotechnological valorisation of cellulose due to re-depositioning on fibrous surfaces. With respect to structural features of the pseudo-lignins, only main functional group contents are normally reported, claiming the presence of ketones, acids, and aromatic structures. [15,53] On the other hand, starting from furfural-derived reactive molecules, also the formation of humins[54–57] has been reported as possibility to valorise biomass-derived carbohydrates.[55]

In light of recent reports which exploited 5-hydroxymethyl furfural (**5-HMF**) and derivatives as crosslinker in lignin-based resins,[20] as well as on the basis of more recent reports on structural features in humins, we hypothesized that the conditions used in the acidic **SE-OS** process for producing lignins **S1** to **S6** would eventually not (only) form pseudo-lignins alongside the initially solubilized and then precipitated lignin. Similarity of conditions generated during fractionation could lead to a the formation of furfural-decorated lignin, or furfural-lignin hybrids, *i.e.*, **FLHs**, and eventually *in extremis* to humin-lignin hybrid polymers, *i.e.*, **HLHs**, and as such severely interfering with downstream valorisations. In the present study, conditions were seen especially suitable in systems with an increased acidity and time-determined severity factor suitable to not only favour degradation of sugars, but also their subsequent reaction in terms of acid-catalysed nucleophilic additions, ring-openings, and acetal formations. Figure 3 shows structural features of 5-HMF and humins,[15–23] identified as key motifs and considered stable enough to be found in the isolated lignin and detectable in spectroscopic analysis.

Humin-linked and -derived structures

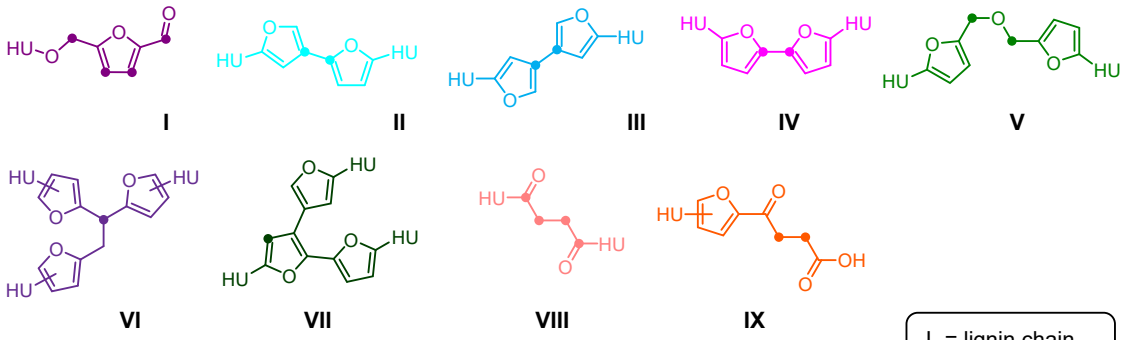

Humin-lignin linkages

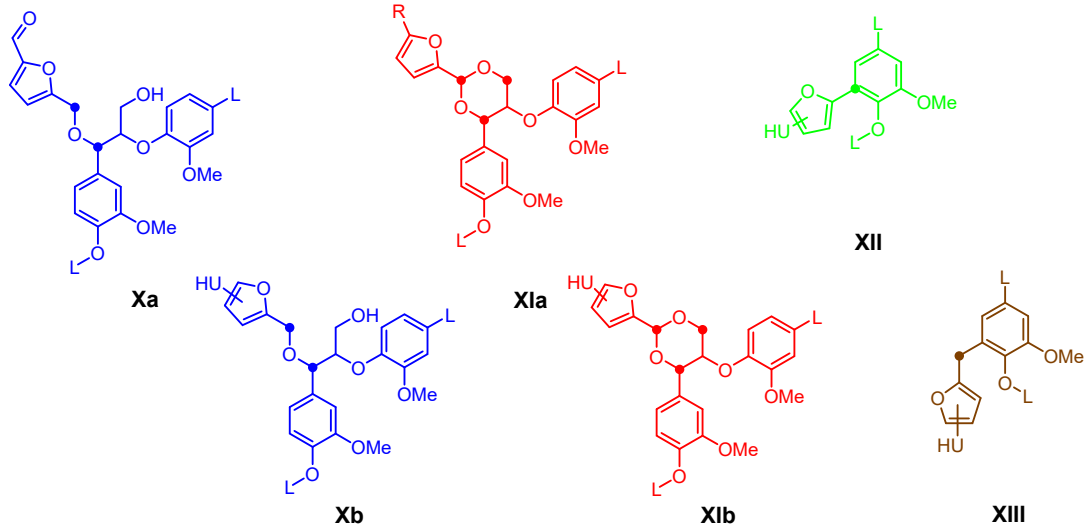

Figure 3. Structural features characteristic for humins (**I** – **IX**), for furfural-lignin hybrids (**FLHs**) (**Xa, XIa**), and for the humin-lignin hybrids (**HLHs**) (**Xb**, **XIb, XII, XIII**).

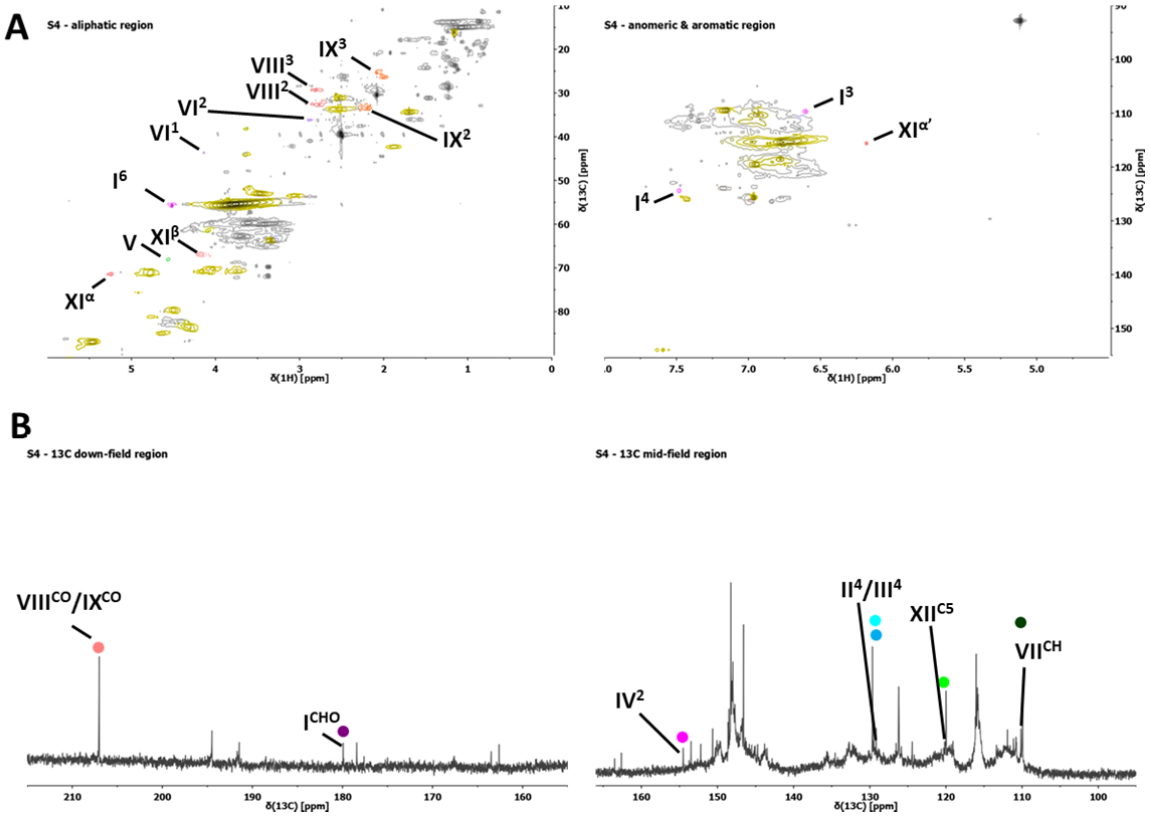

Figure 4. Exemplary visualisation of structural features of humins, furfural-lignin-hybrids (**FLHs**) and humin-lignin hybrids (**HLHs**) in **S4**: (A) HSQC analysis: Colour coding is following Figure 3; structural features of lignins as shown in Figure 2 are shown in yellow, unidentified peaks are kept in grey. (B) ^{13}C NMR analysis: only **FLH**- and **HLH**-related peaks are indicated.

5-HMF-based and –characterising cross-peaks are unambiguously detectable in the HSQC spectra of the isolated lignin fractions (Table 1). **S4** - in terms of lignin structure and absence of carbohydrates appearing as the lignin product of an acceptably functioning fractionation, as long as analyses focuses on lignin and **LCC**-connected cross-peaks and neglects the 'peaks of extractives' – can be used exemplary for showing the relevant cross-peaks in Figure 4, and thus for indicating that such structures are present in lignin samples obtained with process parameters to be considered as viable on the basis of structural features of the isolated lignin (*vide supra*). The intensity of the cross-peak attributable to the furfural aldehyde, detectable in the HSQC at an apparent shift of 9,57|12,7 (δ^1H/[ppm]|δ^{13}C/[ppm]) due to a wrapping of the spectrum, corresponding to real shift of 9.57|177.7 (δ^1H/[ppm]|δ^{13}C/[ppm]) upon unwrapping the spectral data as common in OMICs fields,[58] applying the spectral width of 165 ppm in the carbon domain, amounts to only 0.03 mmol/g in this sample, and is present in the other lignins at higher concentrations (Table 1). this is confirmed by the quantitative ^{13}C NMR analysis, according to which furfural aldehyde is present at a more elevated

level. The presence of these low amounts of furfural cross-peaks, together with the observed decrease of aliphatic OH-groups alongside the increase of aliphatic lignin interunit bonding motif contents suggests an etherification of aliphatic hydroxyls, as suggested in form of structure **Xa** in Figure 3. Considering the average of the furan ring protons in the HSQC, their content amounts to an average of circa 0.44 mmol/g (Table 1). This indicates that the furfural aldehyde, has been partly reduced and/or partly masked as acetal. Corresponding to the latter hypothesis, cross-peaks are delineable in the HSQC spectra of **S4** that would match C^{α} and C^{γ} of a β-O-4' interunit linkage occupied in the formation of an acetal-dioxane motif **XIa**, indicated in Figure 3 as an alternative form of a furfural-lignin hybrid, **FLH**.

Such a relatively stable acetal could be one integral part of a larger covalently linked construct of humin-like structures and lignin molecules, representing a furfural-lignin copolymer or hybrid, **HLH**. The HSQC-derived intensity of the methylene group in a **5-HMF**–based motif (Figure 3) amounts to ca. 0.4 mmol/g (Table 1) indicating in connection with the abundance of C^3-H and C^4-H (Table 1) that parts of the furan content must have undergone oxidative heteroaromatic coupling and oxidative polymerisation *via* the aliphatic side chains. Both features are in agreement with current structural ideas of humins produced in similar chemical environments.[59] Analysis of HSQC and ^{13}C NMR data of **S4** (Figure 4) reveal (cross-)peaks for other typical humin motifs, depicted in Figure 3 as structures **II** –**VII**, and quantified in Table 1.

NMR analyses additionally reveal motifs resulting from an acid-catalysed, hydrolytic ring-opening of furans in **S4** (Figures 3 & 4). Carboxylic acid **IX**, reported as part of humins,[16] is detectable via the α- and β-methylene carbons at 2.46|26.24 and 2.54|33.73(δ^1H/[ppm]|δ^{13}C/[ppm]), respectively (Table 1); the approx. abundance of ca. 1.4 mmol/g is high with respect to the so far discussed furfural and humin signals as impurities. The value does fit, however, the high abundance, found *via* the quantitative ^{13}C NMR, for 'internal' open furans (**VIII**, Figure 3) in terms of carbonyl-flanked ethylene carbons and the flanking ketones (Table 1).

Acids, aldehydes and ketones discussed here as furfural-derived and/or humin-incorporated features could principally also originate from oxidation of the aliphatic hydroxyl groups in the lignin side-chains. The overall aldehyde content is, however, significantly greater than the aldehyde content clearly attributable to lignin motifs (Table 1). Equally, the intensity of the signal attributed to ketone functionalities is greater than the intensity of the one corresponding to α-oxidised β-*O*-4' structures. In combination with the abundances of furan-crosslinking motifs this suggests the presence of larger structures, *i.e.*, humins, giving overall thus rise to covalently linked humin-lignin hybrid (**HLH**) structures not yet described. Even considering a certain overestimation due to peak overlapping and

noise levels in the analysed quantitative ^{13}C NMR, postulating organosolv-born **HLHs** remains reasonable.

Covalent linkages seem not being limited to cyclic acetals or benzylic ethers as discussed above in form of structures **Xb** and **XIb**(Figure 3), but importantly involve additionally direct oxidative phenol-furan coupling. Despite being a softwood lignin sample, ^{31}P NMR suggests a distinct amount of *ortho*-disubstituted phenolics in **S4** (Table 1). This is in line with an oxidative coupling at C^5 with a furan moiety, in form of a weak peak identifiable in the ^{13}C NMR (Figure 4B, Table 1) as typical for a furan C^2 linked to a phenol, *i.e.*, motif **XII** in Figure 3.[17]

Development of functional group contents (Table 1) as function of severity can be rationalised as follows: ketones are present in **S2** and **S4**, with these carbonyl groups being reportedly present in humins, stemming from the hydrolytic opening of the furan motif (*vide supra*).[20] Drastic reduction in ketones upon extending treatment time from **S2** to **S3** could indicate that the 'original' humin structures acts as a reactive scaffold which could cause polymerisation and generation of products becoming insoluble or redeposited, and are thus not visible in material isolated after prolonged treatment times, *i.e.*, 62% isolated **S3.**[54] Increasing intrinsic acidity and reducing time diminishes, but not fully eliminates, the carbonyls in isolated76% of **S4**, rendering this material still soluble enough to be isolated in the applied procedure. Increased acidity by added mineral acids then eliminates carbonyls again in isolated 72% **S5**.

S6 seems to contradict this generalised interpretation due to the high isolation yield of 79%. Yet, looking at the deviations of the various structural motifs as shown in Table 1 relative to **S2**, it becomes apparent that **S6** conditions, though being logically in line with the series, yield overall drastic changes, effectively diminishing significantly carbohydrate-related signals. In other words, decomposition of any organic structure is more effectively achieved here, most probably by not allowing the reactive intermediates to form humins and subsequently **HLHs** as observed for **S4** and **S5**. This can eventually be interpreted as the transition from the presence of humin structures in humin-lignin hybrids, *i.e.*, **HLHs** in **S4**, towards the formation of the previously reported, yet structurally not in detail elucidated pseudo-lignins 'polluting' **S6**. As indicated in Table 1, signals attributable as indicators for pseudo-lignin presences, *i.e.*, an β-CH_2 in an aliphatic aldehyde[60] and a methylene bridging two aromatics,[60] are diminishing alongside, albeit more drastically, when increasing acid content towards **S6** conditions (Table 1). Correspondingly, the former two groups also diminish when increasing intrinsic acidity going from **S3** to **S4** production. Importantly, this indicates that the pseudo-lignins are above all an intermediate product formed during an onset of sugar-degradation. The pseudo-lignin structure 'matures' then as such, maintaining initial motifs in more

polymeric forms yet to be elucidated in detail, becoming humin-like, with the latter being eventually incorporated into lignins in form of **HLHs** as described above when conditions are favourable. Figure 5 summarises the structural discussion in form of a potential mechanistic pathway to the proposed novel **HLHs** as integral and representative structures for the isolated lignins.

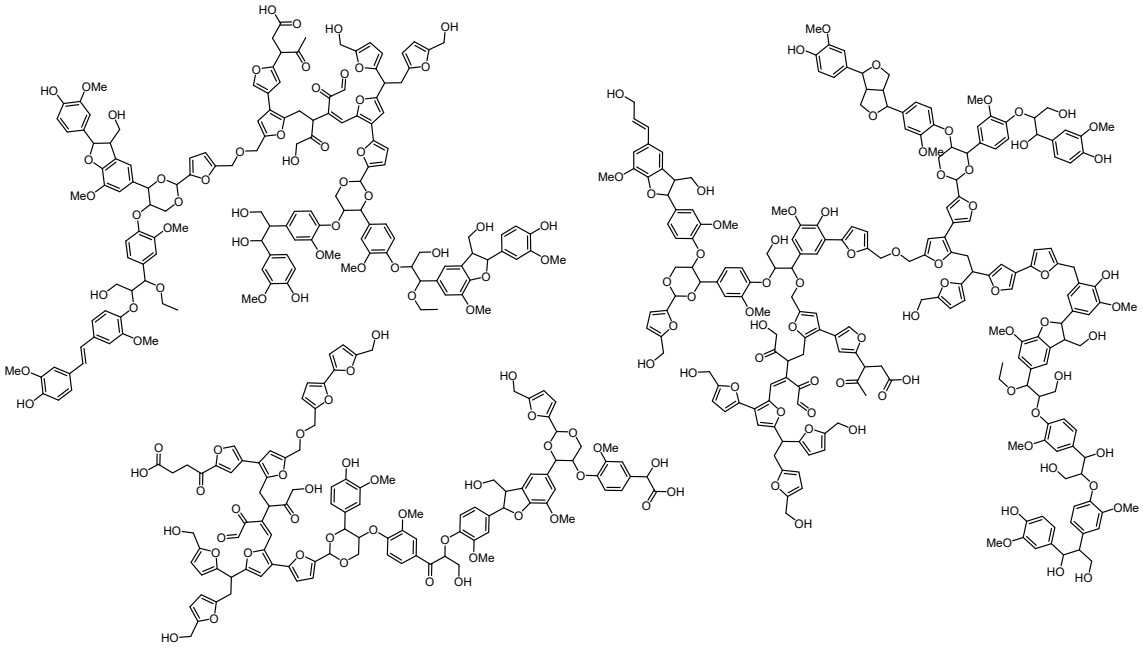

Figure 5. Exemplary structural representations of proposed humin-lignin hybrids, **HLHs**, depicting structural motifs as discussed in the main text. *N.B:* structural representation does not reflect abundancies of a specific sample.

3.6 Thermal analysis of spruce lignins

TGA and dTGA were chosen as relevant characteristics of as lignins that directly reflect structural aspects, and could thus serve as an immediate way of verifying the structural hypothesis and getting hints regarding the consequences they bring with respect to applications.

The chemical alterations observed upon increasing treatment time are reflected in the dTGA and TGA data (Figure 6) for samples **S1**, **S2**, and **S3** (see the Supporting Information for brief reviewing of thermal response behaviours of encountered functional groups.

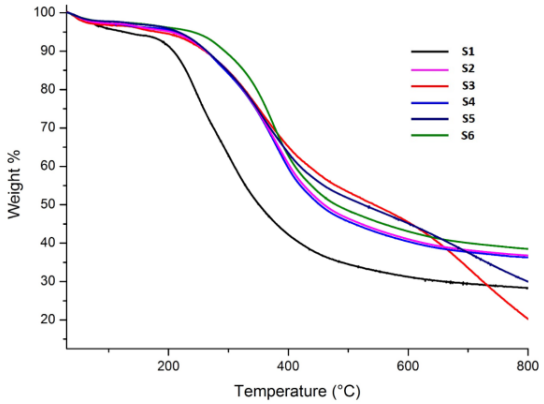

Figure 6. dTGA and TGA of the isolated lignins **S1** – **S6**.

S1, containing residual polysaccharides, is characterized by a rapid onset of thermal degradation at around 200° C, leading to a greater overall mass loss of 10%, which is in-line with the values reported for sugar content in **S1**.[61] Extending treatment times to produce **S2** and **S3**, a gradual change from thermal liability at intermediate temperatures (**S2**) towards higher stability at intermediate temperatures (**S3**) is found, despite some thermal instability in the highest temperature region. As discussed previously,[13] this seems counter-intuitive, as **S3** displays the highest content of liable β-*O*-4' linkages and should thus decompose more readily in the intermediate temperature range. However, the simultaneous introduction of a greater content of aliphatic condensation structures, and thus net reduction in aliphatic OH-groups, can act as structural counterpoise. This trend is additionally aided by i) the reduction in molecular weight; ii) an increase in G-type OH-groups;[62] iii) α-ethoxylation of β-*O*-4' motifs;[63] and iv) α-etherification with furfural and humins as discussed above.

TGA and dTGA data indicate only minor effects on the *overall* thermal stability (*vide infra*) of the above discussed structural changes caused by a reduction on ethanol content going from lignin extracts **S2** to **S4**, causing also only similar char yields for both lignins. Yet, as a small but particularly interesting difference appears a shoulder in the medium temperature region in **S4**.

The gradual change of lignin structure introduced by the acid presence in **S5** and **S6** treatment conditions has a more significant effect. In case of 0.2 % v/v acid catalyst, *i.e.*, **S5**, distinct regions of significant mass loss exist in both the intermediate and the high temperature region around 700° C. For **S6**, *i.e.*, 1 % v/v acid catalyst, only a single mass loss occurs in the intermediate temperature region. S6 seems thus once more to be an outlier at first glance, but **S6** lignin is, however, characterized by the highest char yield (Figure 6). **S6** structures display the largest number and weight average molecular weights across the systems for which a 'time-independent acidity effect'

can be discussed, *i.e.*, **S2**, **S4**, **S5** and **S6**. Yet, an elevated content of thermally liable ether structures such as β-*O*-4' could explain the faster mass loss for **S6** in the intermediate temperature regime remained only to a lower extent in **S6**. The mass loss occurring at low temperatures for **S6** in the intermediate temperature region, in light of the overall highest char yield, thus reflects structural features like the discussed condensed biaryl structures that do not easily generate volatiles, in contrast to the structural features of **S5** and **S4**. Humin-lignin hybrids, **HLHs**, in light of the structural insights discussed for **S4** and **S6**, remain as only significant source of explanation for the observed development of the thermal behaviour. Condensed structures stemming not only from expectable lignin degradation but also from sugar degradation and repolymerisation gradually substitute aliphatic structures responsible for mass loss in moderate temperature regions, causing char yields higher than expected.

4 Conclusion

Various lignins isolated from spruce in a combined steam-explosion – organosolv (**SE-OS**) process were structurally elucidated in detail. Structural features typical for lignins could be detected and related to isolation conditions in terms of direct effects of time and facultative presence of acid-catalyst. The clearly visible presence of additional functional groups typical for sugars, humins and pseudo-lignins in various of the isolated lignins gave rise to a revision of the structural picture of the lignins isolated in this type of process using conditions rather 'standard' in the field and not often questioned. Increasing process severity, especially in terms of acidity, favours the presence of furfural and humin structures in the isolated lignins, in form of also covalently linked humin-lignin hybrids, **HLHs**, that have not yet been described as structural feature yet. These hybrids are characterised by oligomeric and/or polymeric humins linked *via* cyclic acetals and furan-phenol biaryls to lignin oligomers. Pseudo-lignins represent, at least in the chemical space covered in this work, rather an intermediate product emerging from sugar degradation, maturing into humin structures subsequent **HLH**-formation. To the best of the author's knowledge, this work represents one of the first examples in which the worlds of lignins, pseudo-lignins, and humins are joined to arrive at a more holistic view that more realistically considers the complexity of the lignocellulosic biomass during chemical treatments for fractionation. In more practical terms, the work highlights simply the importance of validating process parameters on the basis of a holistic set of analysis techniques.

The demonstrated presence of **HLHs** in **SE-OS** lignins obtained under certain conditions might require a change in the way organosolv lignins are *a priori* seen, or taken for, with the consequences for

various valorisation attempts. As integral, covalently linked part of the organosolv lignin structures that cannot be simply 'washed away' by chromatographic efforts or ultrafiltration, and with rather standard conditions favouring their formation in even not insignificant amounts, they are responsible for, *e.g.*, eventually unexpected solubility issues generally observed in **OS-**lignins, and can explain eventually encountered, unexpected scarce utility of **OS** lignins in some high value-added applications. On the other hand, a purposeful production of HLHs might be a promising starting point to a type of 'one-pot synthesis' of resins so far produced from lignin and furfural additives.

Funding

The work was funded by the Swedish Research Council for Environment, Agricultural Sciences and Spatial Planning (Formas) under grant no 2016-20022.

CRediT authorship contribution statement

Petter Paulsen Thoresen: Investigation, Data acquisition, Data analyses, Writing – Original draft preparation. **Heiko Lange:** Conceptualization, Methodology, Supervision, Data acquisition, Data curation, Writing - Original draft preparation, Writing - Reviewing and Editing. **Ulrika Rova:** Conceptualization, Funding, Supervision. **Paul Christakopoulos:** Conceptualization, Funding, Supervision. **Leonidas Matsakas:** Conceptualization, Methodology, Supervision, Data acquisition, Data curation, Writing - Reviewing and Editing.

Data availability

Data will be made available upon request.

Acknowledgements

All authors would also like to thank Dr. Shubhankar Bhattacharyya (Chemistry of Interfaces, Luleå University of Technology) for his assistance during TGA analysis of lignins. PPT, UR, PC and LM would like to acknowledge Bio4Energy, a strategic research environment provided by the Swedish government, for supporting this work. The contribution of COST Action LignoCOST (CA17128), supported by COST (European Cooperation in Science and Technology), in promoting interaction,

exchange of knowledge and collaborations in the field of lignin valorization is gratefully acknowledged. HL would like to additionally thank the MIUR for the Grant 'Dipartimento di Eccellenza 2019-2022' to the Department of Earth and Environmental Sciences of the University of Milano-Bicocca.

Conflict of interest statement

The authors declare that they have no known competing financial interests or personal relationships that could have appeared to influence the work reported in this paper.

Appendix A. Supporting Information

Supplementary data associated with this article, *i.e.*, additional explanations and figures of HSQC, ^{13}C NMR and FT-IR spectra for lignins **S1** – **S6**, can be found in the online version at doi:10.1016/j.ijbiomac.2022.12345

References

[1] F. H. Isikgor, C. Remzi Becer, Lignocellulosic biomass: a sustainable platform for the production of bio-based chemicals and polymers, Polym Chem. 6 (2015) 4497–4559. https://doi.org/10.1039/C5PY00263J.

[2] Y.-S. Jang, B. Kim, J.H. Shin, Y.J. Choi, S. Choi, C.W. Song, J. Lee, H.G. Park, S.Y. Lee, Bio-based production of C2–C6 platform chemicals, Biotechnol Bioeng. 109 (2012) 2437–2459. https://doi.org/10.1002/BIT.24599.

[3] J. Ralph, C. Lapierre, W. Boerjan, Lignin structure and its engineering, Curr Opin Biotechnol. 56 (2019) 240–249. https://doi.org/10.1016/j.copbio.2019.02.019.

[4] W. Boerjan, J. Ralph, M. Baucher, Lignin Biosynthesis, Annu Rev Plant Biol. 54 (2003) 519–546. https://doi.org/10.1146/annurev.arplant.54.031902.134938.

[5] D. Tarasov, M. Leitch, P. Fatehi, Lignin-carbohydrate complexes: Properties, applications, analyses, and methods of extraction: A review, Biotechnol Biofuels. 11 (2018) 269. https://doi.org/10.1186/s13068-018-1262-1.

[6] A. Dastpak, T. V. Lourençon, M. Balakshin, S. Farhan Hashmi, M. Lundström, B.P. Wilson, Solubility study of lignin in industrial organic solvents and investigation of electrochemical properties of spray-coated solutions, Ind Crops Prod. (2020). https://doi.org/10.1016/j.indcrop.2020.112310.

[7] M. Chadni, N. Grimi, O. Bals, I. Ziegler-Devin, N. Brosse, Steam explosion process for the selective extraction of hemicelluloses polymers from spruce sawdust, Ind Crops Prod. 141 (2019) 111757. https://doi.org/10.1016/J.INDCROP.2019.111757.

[8] M. Muzamal, K. Jedvert, H. Theliander, A. Rasmuson, Structural changes in spruce wood during different steps of steam explosion pretreatment, Holzforschung. 69 (2015) 61–66. https://doi.org/10.1515/HF-2013-0234.

[9] X. Pan, C. Arato, N. Gilkes, D. Gregg, W. Mabee, K. Pye, Z. Xiao, X. Zhang, J. Saddler, Biorefining of softwoods using ethanol organosolv pulping: Preliminary evaluation of process streams for manufacture of fuel-grade ethanol and co-products, Biotechnol Bioeng. 90 (2005) 473–481. https://doi.org/10.1002/BIT.20453.

[10] A. Dastpak, T. v. Lourençon, M. Balakshin, S. Farhan Hashmi, M. Lundström, B.P. Wilson, Solubility study of lignin in industrial organic solvents and investigation of electrochemical properties of spray-coated solutions, Ind Crops Prod. 148 (2020) 112310. https://doi.org/10.1016/J.INDCROP.2020.112310.

[11] F.P. Bouxin, S. David Jackson, M.C. Jarvis, Organosolv pretreatment of Sitka spruce wood: Conversion of hemicelluloses to ethyl glycosides, Bioresour Technol. 151 (2014) 441–444. https://doi.org/10.1016/J.BIORTECH.2013.10.105.

[12] S. Agnihotri, I.A. Johnsen, M.S. Bøe, K. Øyaas, S. Moe, Ethanol organosolv pretreatment of softwood (Picea abies) and sugarcane bagasse for biofuel and biorefinery applications, Wood Science and Technology 2015 49:5. 49 (2015) 881–896. https://doi.org/10.1007/S00226-015-0738-4.

[13] P.P. Thoresen, H. Lange, C. Crestini, U. Rova, L. Matsakas, P. Christakopoulos, Characterization of Organosolv Birch Lignins: Toward Application-Specific Lignin Production, ACS Omega. 6 (2021) 4374–4385. https://doi.org/10.1021/ACSOMEGA.0C05719.

[14] P.P. Thoresen, L. Matsakas, U. Rova, P. Christakopoulos, Recent advances in organosolv fractionation: Towards biomass fractionation technology of the future, Bioresour Technol. 306 (2020) 123189. https://doi.org/10.1016/j.biortech.2020.123189.

[15] F. Hu, S. Jung, A. Ragauskas, Pseudo-lignin formation and its impact on enzymatic hydrolysis, Bioresour Technol. 117 (2012) 7–12. https://doi.org/10.1016/j.biortech.2012.04.037.

[16] C. Cantarutti, R. Dinu, A. Mija, Biorefinery Byproducts and Epoxy Biorenewable Monomers: A Structural Elucidation of Humins and Triglycidyl Ether of Phloroglucinol Cross-Linking, Biomacromolecules. 21 (2020) 517–533. https://doi.org/10.1021/acs.biomac.9b01248.

[17] Y. Zhang, Z. Yuan, C.C. Xu, Engineering biomass into formaldehyde-free phenolic resin for composite materials, AIChE Journal. 61 (2015) 1275–1283. https://doi.org/10.1002/aic.14716.

[18] Y. Zhang, N. Li, Z. Chen, C. Ding, Q. Zheng, J. Xu, Q. Meng, Synthesis of High-Water-Resistance Lignin-Phenol Resin Adhesive with Furfural as a Crosslinking Agent, Polymers (Basel). 12 (2020) 2805. https://doi.org/10.3390/polym12122805.

[19] C. Falco, F. Perez Caballero, F. Babonneau, C. Gervais, G. Laurent, M.M. Titirici, N. Baccile, Hydrothermal carbon from biomass: Structural differences between hydrothermal and pyrolyzed carbons via 13C solid state NMR, Langmuir. 27 (2011) 14460–14471. https://doi.org/10.1021/la202361p.

[20] X. Zhu, B. Bruijnaers, T. v. Lourençon, M. Balakshin, Structural Analysis of Lignin-Based Furan Resin, Materials. 15 (2022) 350. https://doi.org/10.3390/ma15010350.

[21] D. Graiver, G.T. Decker, Y. Kim, F.J. Hamilton, H.J. Harwood, Graft and block copolymers with polysiloxane and vinyl polymer segments, Silicon Chemistry. 1 (2002) 107–120. https://doi.org/10.1023/A:1020605128180.

[22] R. Rego, P.J. Adriaensens, R.A. Carleer, J.M. Gelan, Fully quantitative carbon-13 NMR characterization of resol phenol-formaldehyde prepolymer resins, Polymer (Guildf). 45 (2004) 33–38. https://doi.org/10.1016/j.polymer.2003.10.078.

[23] Y. Cheng, G. Sui, Synthesis and regulation mechanism of bio-oil–glucose phenolic resin using furfural as cross-linking agent, Iranian Polymer Journal (English Edition). 31 (2022) 619–628. https://doi.org/10.1007/s13726-022-01022-2.

[24] J.L. Wen, B.L. Xue, F. Xu, R.C. Sun, Unveiling the Structural Heterogeneity of Bamboo Lignin by In Situ HSQC NMR Technique, Bioenergy Res. 5 (2012) 886–903. https://doi.org/10.1007/s12155-012-9203-5.

[25] L. Zhang, G. Gellerstedt, Quantitative 2D HSQC NMR determination of polymer structures by selecting suitable internal standard references, Magnetic Resonance in Chemistry. 45 (2007) 37–45. https://doi.org/10.1002/mrc.1914.

[26] S. Bauer, H. Sorek, V.D. Mitchell, A.B. Ibáñez, D.E. Wemmer, Characterization of Miscanthus giganteus lignin isolated by ethanol organosolv process under reflux condition, J Agric Food Chem. (2012). https://doi.org/10.1021/jf302409d.

[27] T.Q. Yuan, S.N. Sun, F. Xu, R.C. Sun, Characterization of lignin structures and lignin-carbohydrate complex (LCC) linkages by quantitative 13C and 2D HSQC NMR spectroscopy, J Agric Food Chem. 59 (2011) 10604–10614. https://doi.org/10.1021/jf2031549.

[28] C. Crestini, H. Lange, M. Sette, D.S. Argyropoulos, On the structure of softwood kraft lignin, Green Chemistry. 19 (2017) 4104–4121. https://doi.org/10.1039/c7gc01812f.

[29] T.Q. Yuan, S.N. Sun, F. Xu, R.C. Sun, Characterization of lignin structures and lignin-carbohydrate complex (LCC) linkages by quantitative 13C and 2D HSQC NMR spectroscopy, J Agric Food Chem. 59 (2011) 10604–10614. https://doi.org/10.1021/jf2031549.

[30] A. Brandt, L. Chen, B.E. van Dongen, T. Welton, J.P. Hallett, Structural changes in lignins isolated using an acidic ionic liquid water mixture, Green Chemistry. 17 (2015) 5019–5034. https://doi.org/10.1039/c5gc01314c.

[31] H.N. Zhang, H. Ren, H.M. Zhai, Analysis of phenolation potential of spruce kraft lignin and construction of its molecular structure model, Ind Crops Prod. 167 (2021) 113506. https://doi.org/10.1016/j.indcrop.2021.113506.

[32] D.J. Yelle, D. Wei, J. Ralph, K.E. Hammel, Multidimensional NMR analysis reveals truncated lignin structures in wood decayed by the brown rot basidiomycete Postia placenta, Environ Microbiol. 13 (2011) 1091–1100. https://doi.org/10.1111/j.1462-2920.2010.02417.x.

[33] R. el Hage, N. Brosse, L. Chrusciel, C. Sanchez, P. Sannigrahi, A. Ragauskas, Characterization of milled wood lignin and ethanol organosolv lignin from miscanthus, Polym Degrad Stab. 94 (2009) 1632–1638. https://doi.org/10.1016/j.polymdegradstab.2009.07.007.

[34] P. Sannigrahi, A.J. Ragauskas, S.J. Miller, Lignin structural modifications resulting from ethanol organosolv treatment of Loblolly pine, Energy and Fuels. 24 (2010) 683–689. https://doi.org/10.1021/ef900845t.

[35] Y. Xie, S. Yasuda, H. Wu, H. Liu, Analysis of the structure of lignin-carbohydrate complexes by the specific 13C tracer method, Journal of Wood Science. 46 (2000) 130–136. https://doi.org/10.1007/BF00777359.

[36] M. Bardet, M.F. Foray, D. Robert, USE OF THE DEPT PULSE SEQUENCE TO FACILITATE THE **1**3C NMR STRUCTURAL ANALYSIS OF LIGNINS., in: 1985: pp. 21–22. https://doi.org/10.1002/macp.1985.021860716.

[37] H. Nishimura, A. Kamiya, T. Nagata, M. Katahira, T. Watanabe, Direct evidence for α ether linkage between lignin and carbohydrates in wood cell walls, Sci Rep. 8 (2018). https://doi.org/10.1038/s41598-018-24328-9.

[38] Y. Miyagawa, Y. Tobimatsu, P.Y. Lam, T. Mizukami, S. Sakurai, H. Kamitakahara, T. Takano, Possible mechanisms for the generation of phenyl glycoside-type lignin–carbohydrate linkages in lignification with monolignol glucosides, Plant Journal. 104 (2020) 156–170. https://doi.org/10.1111/tpj.14913.

[39] Y. Cheng, G. Sui, Synthesis and regulation mechanism of bio-oil–glucose phenolic resin using furfural as cross-linking agent, Iranian Polymer Journal (English Edition). 31 (2022) 619–628. https://doi.org/10.1007/s13726-022-01022-2.

[40] L. Matsakas, V. Raghavendran, O. Yakimenko, G. Persson, E. Olsson, U. Rova, L. Olsson, P. Christakopoulos, Lignin-first biomass fractionation using a hybrid organosolv – Steam explosion pretreatment technology improves the saccharification and fermentability of spruce biomass, Bioresour Technol. 273 (2019) 521–528. https://doi.org/10.1016/j.biortech.2018.11.055.

[41] L. Mu, J. Wu, L. Matsakas, M. Chen, U. Rova, P. Christakopoulos, J. Zhu, Y. Shi, Two important factors of selecting lignin as efficient lubricating additives in poly (ethylene glycol): Hydrogen bond and molecular weight, Int J Biol Macromol. 129 (2019) 564–570. https://doi.org/10.1016/j.ijbiomac.2019.01.175.

[42] M.N. Muraleedharan, D. Zouraris, A. Karantonis, E. Topakas, M. Sandgren, U. Rova, P. Christakopoulos, A. Karnaouri, Effect of lignin fractions isolated from different biomass sources on cellulose oxidation by fungal lytic polysaccharide monooxygenases, Biotechnol Biofuels. 11 (2018). https://doi.org/10.1186/s13068-018-1294-6.

[43] N. Giummarella, L. Zhang, G. Henriksson, M. Lawoko, Structural features of mildly fractionated lignin carbohydrate complexes (LCC) from spruce, RSC Adv. 6 (2016) 42120–42131. https://doi.org/10.1039/c6ra02399a.

[44] X. Zhong, R. Yuan, B. Zhang, B. Wang, Y. Chu, Z. Wang, Full fractionation of cellulose, hemicellulose, and lignin in pith-leaf containing corn stover by one-step treatment using aqueous formic acid, Ind Crops Prod. 172 (2021). https://doi.org/10.1016/j.indcrop.2021.113962.

[45] D.S. Zijlstra, C.W. Lahive, C.A. Analbers, M.B. Figueirêdo, Z. Wang, C.S. Lancefield, P.J. Deuss, Mild Organosolv Lignin Extraction with Alcohols: The Importance of Benzylic Alkoxylation, ACS Sustain Chem Eng. (2020). https://doi.org/10.1021/acssuschemeng.9b07222.

[46] J. v. Vermaas, M.F. Crowley, G.T. Beckham, A Quantitative Molecular Atlas for Interactions between Lignin and Cellulose, ACS Sustain Chem Eng. 7 (2019) 19570–19583. https://doi.org/10.1021/acssuschemeng.9b04648.

[47] C. Zhang, X. Yang, Molecular dynamics simulation of ethanol/water mixtures for structure and diffusion properties, Fluid Phase Equilib. 231 (2005) 1–10. https://doi.org/10.1016/J.FLUID.2005.03.018.

[48] M. Matsumoto, N. Nishi, T. Furusawa, M. Saita, T. Takamuku, M. Yamagami, T. Yamaguchi, Structure of Clusters in Ethanol–Water Binary Solutions Studied by Mass Spectrometry and X-Ray Diffraction, Bull Chem Soc Jpn. 68 (1995) 1775–1783. https://doi.org/10.1246/BCSJ.68.1775.

[49] P. Creux, J. Lachaise, A. Graciaa, J.K. Beattie, A.M. Djerdjev, Strong Specific Hydroxide Ion Binding at the Pristine Oil/Water and Air/Water Interfaces, Journal of Physical Chemistry B. 113 (2009) 14146–14150. https://doi.org/10.1021/JP906978V.

[50] S. Agnihotri, I.A. Johnsen, M.S. Bøe, K. Øyaas, S. Moe, Ethanol organosolv pretreatment of softwood (Picea abies) and sugarcane bagasse for biofuel and biorefinery applications, Wood Sci Technol. 49 (2015) 881–896. https://doi.org/10.1007/s00226-015-0738-4.

[51] J.H. Choi, S.K. Jang, J.H. Kim, S.Y. Park, J.C. Kim, H. Jeong, H.Y. Kim, I.G. Choi, Simultaneous production of glucose, furfural, and ethanol organosolv lignin for total utilization of high recalcitrant biomass by organosolv pretreatment, Renew Energy. 130 (2019) 952–960. https://doi.org/10.1016/j.renene.2018.05.052.

[52] J. Wildschut, A.T. Smit, J.H. Reith, W.J.J. Huijgen, Ethanol-based organosolv fractionation of wheat straw for the production of lignin and enzymatically digestible cellulose, Bioresour Technol. 135 (2013) 58–66. https://doi.org/10.1016/j.biortech.2012.10.050.

[53] W.C. Tu, J.P. Hallett, Recent advances in the pretreatment of lignocellulosic biomass, Curr Opin Green Sustain Chem. 20 (2019) 11–17. https://doi.org/10.1016/J.COGSC.2019.07.004.

[54] G. Wan, Q. Zhang, M. Li, Z. Jia, C. Guo, B. Luo, S. Wang, D. Min, How Pseudo-lignin Is Generated during Dilute Sulfuric Acid Pretreatment, J Agric Food Chem. 67 (2019) 10116–10125. https://doi.org/10.1021/ACS.JAFC.9B02851.

[55] I. van Zandvoort, Y. Wang, C.B. Rasrendra, E.R.H. van Eck, P.C.A. Bruijnincx, H.J. Heeres, B.M. Weckhuysen, Formation, Molecular Structure, and Morphology of Humins in Biomass Conversion: Influence of Feedstock and Processing Conditions, ChemSusChem. 6 (2013) 1745–1758. https://doi.org/10.1002/cssc.201300332.

[56] M. Sajid, M. Rizwan Dilshad, M. Saif Ur Rehman, D. Liu, X. Zhao, Catalytic Conversion of Xylose to Furfural by p-Toluenesulfonic Acid (pTSA) and Chlorides: Process Optimization and Kinetic Modeling, Molecules. 26 (2021) 2208. https://doi.org/10.3390/molecules26082208.

[57] F. Delbecq, Y. Wang, C. Len, Conversion of xylose, xylan and rice husk into furfural via betaine and formic acid mixture as novel homogeneous catalyst in biphasic system by microwave-assisted dehydration, J Mol Catal A Chem. 423 (2016) 520–525. https://doi.org/10.1016/j.molcata.2016.07.003.

[58] I.A. Lewis, M.R. Shortreed, A.D. Hegeman, J.L. Markley, Novel NMR and MS approaches to metabolomics, Methods in Pharmacology and Toxicology. 17 (2012) 199–230. https://doi.org/10.1007/978-1-61779-618-0_7.

[59] I. van Zandvoort, E. J. Koers, Markus Weingarth, P.C. A. Bruijnincx, Marc Baldus, B. M. Weckhuysen, Structural characterization of 13 C-enriched humins and alkali-treated 13 C humins by 2D solid-state NMR, Green Chemistry. 17 (2015) 4383–4392. https://doi.org/10.1039/C5GC00327J.

[60] B. Cheng, X. Wang, Q. Lin, X. Zhang, L. Meng, R.-C. Sun, F. Xin, J. Ren, New Understandings of the Relationship and Initial Formation Mechanism for Pseudo-lignin, Humins, and Acid-Induced Hydrothermal Carbon, (2018). https://doi.org/10.1021/acs.jafc.8b04754.

[61] L. Matsakas, V. Raghavendran, O. Yakimenko, G. Persson, E. Olsson, U. Rova, L. Olsson, P. Christakopoulos, Lignin-first biomass fractionation using a hybrid organosolv – Steam explosion pretreatment technology improves the saccharification and fermentability of spruce biomass, Bioresour Technol. 273 (2019) 521–528. https://doi.org/10.1016/j.biortech.2018.11.055.

[62] J.-H. Choi, S.-M. Cho, J.-C. Kim, S.-W. Park, Y.-M. Cho, B. Koo, H.W. Kwak, I.-G. Choi, Thermal Properties of Ethanol Organosolv Lignin Depending on Its Structure, ACS Omega. 6 (2021) 1534–1546. https://doi.org/10.1021/ACSOMEGA.0C05234.

[63] L. Yin, E. Leng, X. Gong, Y. Zhang, X. Li, Pyrolysis mechanism of β-O-4 type lignin model polymers with different oxygen functional groups on Cα, J Anal Appl Pyrolysis. 136 (2018) 169–177. https://doi.org/10.1016/J.JAAP.2018.10.008.

Table of content text and image

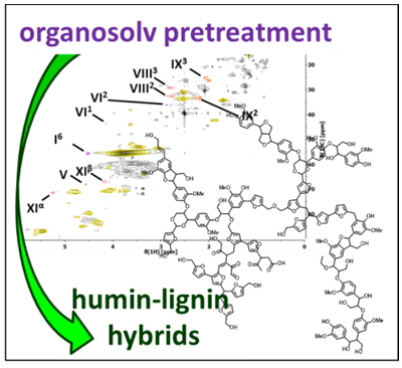

Careful structural analyses of spruce organosolv lignin isolates by state-of-the-art techniques revealed a new structural component: humin-lignin hybrids. These novel structures can help to understand the complex interplay between the structural polymers during common biorefinery approaches, and can explain puzzling physico-chemical behaviours of organosolv lignins.